

See discussions, stats, and author profiles for this publication at: <https://www.researchgate.net/publication/258957045>

Four-Component Relativistic DFT Calculations of NMR Shielding Tensors for Paramagnetic Systems.

ARTICLE in THE JOURNAL OF PHYSICAL CHEMISTRY A · NOVEMBER 2013

Impact Factor: 2.69 · DOI: 10.1021/jp408389h · Source: PubMed

CITATIONS

13

READS

98

5 AUTHORS, INCLUDING:



[Stanislav Komorovský](#)

University of Tromsø

28 PUBLICATIONS 333 CITATIONS

SEE PROFILE



[Michal Repisky](#)

University of Tromsø

34 PUBLICATIONS 417 CITATIONS

SEE PROFILE



[Kenneth Ruud](#)

University of Tromsø

343 PUBLICATIONS 8,675 CITATIONS

SEE PROFILE



[Olga L Malkina](#)

Slovak Academy of Sciences

87 PUBLICATIONS 4,231 CITATIONS

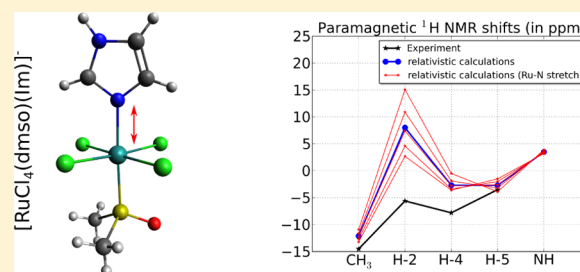
SEE PROFILE

Four-Component Relativistic Density Functional Theory Calculations of NMR Shielding Tensors for Paramagnetic Systems

Stanislav Komorovsky,^{*,†,‡} Michal Repisky,^{†,‡} Kenneth Ruud,[†] Olga L. Malkina,[‡] and Vladimir G. Malkin[‡][†]Centre for Theoretical and Computational Chemistry, University of Tromsø—The Arctic University of Norway, N-9037 Tromsø, Norway[‡]Institute of Inorganic Chemistry, Slovak Academy of Sciences, Dúbravská cesta 9, SK-84536 Bratislava, Slovakia

ABSTRACT: A four-component relativistic method for the calculation of NMR shielding constants of paramagnetic doublet systems has been developed and implemented in the ReSPECT program package. The method uses a Kramer unrestricted noncollinear formulation of density functional theory (DFT), providing the best DFT framework for property calculations of open-shell species. The evaluation of paramagnetic nuclear magnetic resonance (pNMR) tensors reduces to the calculation of electronic \mathbf{g} tensors, hyperfine coupling tensors, and NMR shielding tensors. For all properties, modern four-component formulations were adopted.

The use of both restricted kinetically and magnetically balanced basis sets along with gauge-including atomic orbitals ensures rapid basis-set convergence. These approaches are exact in the framework of the Dirac–Coulomb Hamiltonian, thus providing useful reference data for more approximate methods. Benchmark calculations on Ru(III) complexes demonstrate good performance of the method in reproducing experimental data and also its applicability to chemically relevant medium-sized systems. Decomposition of the temperature-dependent part of the pNMR tensor into the traditional contact and pseudocontact terms is proposed.



1. INTRODUCTION

Nuclear magnetic resonance (NMR) spectroscopy is routinely used in many areas of chemical research.¹ Although the vast majority of studies deal with diamagnetic systems, the NMR of paramagnetic substances (pNMR) is becoming crucial in many areas of research, for example, in the development of new magnetic materials^{2,3} or in studies of biological systems.^{4,5} Bertini et al.⁴ note that a third of all proteins are metalloproteins, and a significant number of these metalloproteins are paramagnetic. It is therefore reasonable to expect growth in the importance of pNMR, especially in view of recent pNMR instrumental improvements.⁶ In turn, this requires new theoretical approaches for the analysis and interpretation of experimental data. It would also be very desirable to assess the accuracy of the approximations currently used in experimental studies and to propose better shift–structure relationships.

It is customary to decompose the pNMR shift of nucleus M into three contributions (here we will restrict ourselves to the isotropic part of the pNMR tensor):⁷

$$\delta_M = \delta_M^{\text{orb}} + \delta_M^{\text{fc}} + \delta_M^{\text{pc}} \quad (1)$$

where δ_M^{orb} , δ_M^{fc} , and δ_M^{pc} denote the orbital, contact, and pseudocontact shifts, respectively. In theoretical calculations, based on the Ramsey theory of NMR^{8,9} (see also ref 10 and references therein), the orbital shift δ_M^{orb} is evaluated as the difference between the chemical shielding of some reference compound and the orbital contribution to the shielding tensor of the investigated paramagnetic systems:

$$\delta_M^{\text{orb}} = \sigma_M^{\text{ref}} - \sigma_M^{\text{orb}} \quad (2)$$

The orbital contribution is approximately temperature-independent (if the vibrational motion of the nuclei is neglected), and in both theoretical as well as experimental studies it is usually approximated by the NMR shift of the diamagnetic analogue of the molecular system. To avoid this approximation in experimental studies, the temperature-(in)-dependent parts of eq 1 can be separated by a least-squares fit ($1/T$ dependence) of NMR spectra measured at different temperatures. From this fit, it is also possible to assign the measured NMR signals to the shielding constants of individual nuclei. However, this approach requires precise measurements of pNMR shifts over a wide temperature range, and its applicability is therefore somewhat limited.

The contact and pseudocontact terms^{7,11,12} in eq 1 are temperature-dependent, and they appear in addition to the usual Ramsey orbital term only if more states than one are populated. These terms are therefore unique for paramagnetic systems. In the simplest case, when the system obeys the Curie law [i.e., in the absence of zero-field splitting (ZFS) and when the $(2S + 1)$ degenerate ground state is well-separated from excited energy levels], the contact shift obeys the relation:¹¹

Received: August 21, 2013

Revised: November 26, 2013

Published: November 27, 2013



$$\delta_M^{\text{fc}} = \frac{\mu_e}{\gamma_M} \frac{S(S+1)}{3kT} g^{\text{iso}} A_M^{\text{iso}} \quad (3)$$

where μ_e is the Bohr magneton, γ_M is the gyromagnetic ratio of nucleus M, kT is the thermal energy, $(2S+1)$ is the multiplicity of the ground state, g^{iso} is the isotropic part of the \mathbf{g} tensor, and A_M^{iso} is the isotropic part of the hyperfine coupling tensor. In this particular case, the contact shift originates from the isotropic hyperfine interaction, which is represented in nonrelativistic theory by the Fermi contact operator (hence the term contact shift), and the “averaged electron spin at the position of the nucleus”.⁴ The contact shift in this approximate form can therefore be used to extract the spin density at nucleus M (see ref 3 and references therein).

If the electron spin on the paramagnetic center can be considered as a point dipole (with respect to the measured nucleus) and if the studied system obeys the Curie law, the pseudocontact shift can be evaluated as¹²

$$\delta_M^{\text{pc}} = \frac{\mu_e}{\gamma_M} \frac{S(S+1)}{9kT} \text{Tr}(\mathbf{g}^{\text{ani}} \mathbf{A}_M^{\text{dip}}) \quad (4)$$

where \mathbf{g}^{ani} denotes the \mathbf{g} -tensor anisotropy and $\mathbf{A}_M^{\text{dip}}$ is the dipolar part of the hyperfine coupling tensor. Equation 4 can be written in different forms.^{4,7,12} We have chosen the form that is consistent with the theory presented in section 2. The pseudocontact shift can be rationalized as the dipolar interaction between an averaged electron magnetic moment (typically centered on the metal center) and the magnetic moment of the nucleus of interest. From the experimental point of view, the pseudocontact shift contains useful structural information and can help, for example, to determine the structure of metalloproteins (see refs 4 and 5 and references therein).

Although these simple models for pNMR have been applied successfully for more than 50 years, modern quantum-chemical methods have during the past decades gradually been abandoning many of the assumptions and approximations invoked in the derivation of the pNMR shielding constant. This started in 2003 when Rinkevicius et al.¹³ calculated the orbital term directly for paramagnetic systems. They calculated the corresponding quantities only to the lowest order in the fine-structure constant c^{-2} [often referred to as the nonrelativistic (NR) limit], thus neglecting the spin–orbit (SO) as well as scalar relativistic (SR) corrections to the shielding constant. Due to these approximations, they were not able to obtain the isotropic pseudocontact shift. Therefore the method could be applied only to systems containing light elements¹⁴ with large gaps between the highest occupied molecular orbital (HOMO) and the lowest unoccupied molecular orbital (LUMO), because the SO effect otherwise can be big even for a relatively light system.¹⁵

A new chapter in the development of computational approaches for pNMR came with the work of Moon and Patchkovskii,¹⁶ where the authors presented a modern theory of the pNMR shift (recently an alternative theory was proposed by Van Den Heuvel and Soncini^{17,18}). Inspired by the work of Moon and Patchkovskii, Pennanen and Vaara,^{19–21} and Hrobárik et al.²² formulated a theory that also includes relativistic spin–orbit corrections to the calculated pNMR shifts. These effects were formulated consistently to order c^{-4} , by use of a perturbation theory based on the Breit–Pauli Hamiltonian.²³ However, in the actual calculations some of the

SO terms were calculated approximately by an atomic mean-field approach (AMFI).²⁴ Moreover, all SO operators contributing to the orbital shift in eq 2 were neglected, except for the calculation of the diamagnetic reference value in the work of Hrobárik et al.,²² who used a third-order perturbation theory to include these corrections.^{25–27}

A popular way to include relativistic effects in calculations is to use the zero-order regular approximation (ZORA).²⁸ In contrast to the Breit–Pauli perturbation theory just described, the wave function obtained by use of the ZORA Hamiltonian contains scalar and spin–orbit effects from the outset. However, since all efficient ZORA implementations use an atomic approximation to the potential in the ZORA kinetic energy term,^{29,30} all two-electron scalar and SO interactions originating from the Coulomb interaction are approximate (such as the spin–same–orbit²³ contribution) and all two-electron terms arising from the Gaunt interaction (such as the spin–other–orbit²³ contribution) are neglected. These approximations can lead to significant errors in the \mathbf{g} tensor calculations (up to 25–30% for light-element compounds and about 10% for compounds containing heavy elements).³¹ The first calculations of pNMR shifts based on the ZORA Hamiltonian were performed by Rastrelli and Bagno.³² They used eq 3 and an analogue of eq 4 (based on the susceptibility tensor) to calculate the contact and pseudocontact isotropic shift, respectively. Autschbach et al.³³ revised some of the isotropic pNMR shifts from ref 32, noticing in particular the importance of a spin-unrestricted formalism for the calculation of \mathbf{g} and hyperfine coupling tensors and the unsatisfactory quality of the pseudocontact shift estimates from the susceptibility tensor. Recently, Autschbach et al.^{34,35} used the theory of Moon and Patchkovskii¹⁶ to calculate pNMR shifts. In their implementation, one-electron scalar relativistic effects were included variationally in the unperturbed wave function, whereas the SO effects were added as a perturbation in calculations of the hyperfine coupling and \mathbf{g} tensors. However, the SO corrections were omitted in the calculation of the orbital contribution to the pNMR shift (eq 1).

From this brief review of the developments made in the calculation of pNMR shifts during the past decade, we note that all available methods involve (sometimes significant) approximations to the fully relativistic approach for calculating pNMR, restricting the applicability of these methods to only the upper rows of the periodic table. Even in the case of light elements, one must be very careful when omitting relativistic SO effects. Since pNMR spectroscopy by default treats systems with higher spin multiplicity, special care must be taken to properly incorporate SO effects even for systems containing relatively light elements. To illustrate this, let us note that in a system without any SO interaction, the anisotropy of the \mathbf{g} tensor will vanish, making the pseudocontact isotropic shift zero (eq 4), and therefore no structural information will be obtained. This is in clear contradiction with experimental observations, where the pseudocontact shift is used to obtain structural information in metalloproteins.^{4,5}

Here we present an efficient density functional theory (DFT) approach to the calculation of pNMR shifts based on the full Dirac–Coulomb Hamiltonian, thus lifting most of the approximations described above, and relying on our long-standing experience with four-component calculations of electron paramagnetic resonance (EPR) and NMR parameters.^{36–43} Our aim is not only to provide useful data against which other more approximate methods can be benchmarked

but also to demonstrate the applicability of the current implementation to systems of chemical interest. For this purpose we have chosen two Ru(III) complexes previously studied in the work of Rastrelli and Bagno.³² Both complexes have been studied experimentally [meridional isomer of tris(maltolato)ruthenium, *mer*-Ru(ma)₃,⁴⁴ and a new anti-tumor metastasis inhibitor, *trans*-(dimethyl sulfoxide)-(imidazole) tetrachlororuthenate(III), NAMI⁴⁵] and they are also interesting because of their potential medical applications. Note that our goal here is to compare our approach with previous relativistic calculations rather than a detailed analysis of the experimental data.

In this work, we will apply our method to the study of effective doublet systems, consequently avoiding systems with ZFS effects (in contrast to refs 17, 18 and 20–22, where such effects were included). In a forthcoming publication, we will extend the approach presented here to systems with non-zero ZFS.

The remainder of the paper is organized as follows. In section 2 we present the theory of our relativistic four-component DFT approach to the calculation of pNMR shifts. In section 3 we describe the computational details, and the results of our calculations are reported in section 4. Concluding remarks and an outlook are given in section 5.

2. THEORY

Let us consider a paramagnetic system in an external magnetic field \vec{B} . Because of the electrons, nucleus M in this system experiences a local magnetic field different from \vec{B} . In NMR spectroscopy, the interaction of this electron-induced magnetic field and the magnetic moment $\vec{\mu}^M$ of nucleus M is measured and quantified in terms of the shielding constant. In diamagnetic systems, the NMR shielding tensor is the bilinear derivative of the energy of the nondegenerate ground state with respect to the perturbations \vec{B} and $\vec{\mu}^M$. An important feature of paramagnetic systems is that, under experimental conditions (in the presence of an external magnetic field), there is more than one thermally accessible state, including both the Zeeman-split ground state and other low-lying excited states. The energy of the system in thermal equilibrium must then be averaged over the ensemble of these states. The pNMR shielding tensor can then be expressed as follows:^{7,16,17}

$$\sigma_{uv}^M = \left. \frac{\partial^2 \langle E(\vec{B}, \vec{\mu}^M) \rangle}{\partial B_u \partial \mu_v^M} \right|_{\vec{B}=\vec{\mu}^M=0} \quad (5)$$

where $\langle E(\vec{B}, \vec{\mu}^M) \rangle$ denotes the thermal average of the energy and B_u and μ_v^M are Cartesian components of vectors \vec{B} and $\vec{\mu}^M$, respectively. In this work, we will consider only the simplest case where, in the absence of an external magnetic field, all excited states are well separated from the doubly degenerate ground state. Although there exist two different ways of deriving the pNMR shielding tensor within these assumptions,^{16–18} here we follow the work of Van den Heuvel and Soncini,^{17,18} as this approach does not require symmetrization of the \mathbf{g} tensor, $\mathbf{G} = \mathbf{g}\mathbf{g}^T$, and it is thus more general. The paramagnetic NMR shielding tensor then reads

$$\sigma^M = \sigma_M^{\text{orb}} - \frac{\mu_e}{4\gamma_M kT} \mathbf{g} \mathbf{A}_M^T \quad (6)$$

where $(\sigma_M^{\text{orb}})_{uv}$, g_{ut} and $(A_M)_{vt}$ are components of the NMR shielding tensor, \mathbf{g} tensor, and hyperfine coupling (HFC)

tensor of nucleus M , respectively, indices u, v are the same as in eq 5, and t is a Cartesian component of an effective spin operator \hat{S}_{eff} . We note that all assumptions needed for deriving eq 6 also hold for the Dirac–Coulomb Hamiltonian that we are going to use in this work, and in particular the time-reversal symmetry of the relativistic operators.

σ_M^{orb} in eq 6 is the usual NMR shielding tensor known from Ramsey's theory^{8,9} with the difference that the reference wave function is one of the Kramer states. We will refer to σ_M^{orb} as the orbital contribution to the pNMR shielding tensor, and we will use it to obtain the orbital part of the pNMR shift in eq 2.

In relativistic theory, there is an ambiguity in the separation of the second term on the right-hand side of eq 6 into contact and pseudocontact contributions (eq 1). This ambiguity is already observed when perturbation theory is used.^{19,22} In the four-component relativistic theory, the separation will become even more difficult since relativistic effects are included variationally in the four-component wave function. Therefore, one can ensure only the correct nonrelativistic limit for this separation. To achieve such a separation, we follow the work of Bertini et al.,⁴ where the contact pNMR tensor depends on the isotropic Fermi contact contribution to the HFC tensor and the orientation-dependent induced electron magnetic moment,^{7,46} and the pseudocontact pNMR tensor involves the traceless dipole interaction operator (see the definitions in eqs 10 and 11).

Let us first decompose the HFC and \mathbf{g} tensors into isotropic and anisotropic parts:

$$\mathbf{X} = X^{\text{iso}} \mathbf{1} + \mathbf{X}^{\text{ani}} \quad (7)$$

$$X^{\text{iso}} \equiv \frac{1}{3} \text{Tr}[\mathbf{X}] \quad (8)$$

$$\mathbf{X}^{\text{ani}} \equiv \mathbf{X} - X^{\text{iso}} \mathbf{1} \quad (9)$$

In the spirit of the above discussion, we use this decomposition of the hyperfine coupling tensor into the isotropic and anisotropic parts as a guideline for separation of contact and pseudocontact contributions to the pNMR shift tensor:

$$\delta_M^{\text{fc}} = \frac{\mu_e}{4\gamma_M kT} \mathbf{g} \mathbf{A}_M^{\text{iso}} \quad (10)$$

$$\delta_M^{\text{pc}} = \frac{\mu_e}{4\gamma_M kT} \mathbf{g} \mathbf{A}_M^{\text{ani}, T} \quad (11)$$

with the isotropic part

$$\delta_M^{\text{fc}} = \frac{\mu_e}{4\gamma_M kT} \mathcal{S}^{\text{iso}} A_M^{\text{iso}} \quad (12)$$

$$\delta_M^{\text{pc}} = \frac{\mu_e}{12\gamma_M kT} \text{Tr}(\mathbf{g}^{\text{ani}} \mathbf{A}_M^{\text{ani}, T}) \quad (13)$$

Note that the conventional equations for the isotropic part of the pNMR shift (eqs 3 and 4) are consistent with the definitions in eqs 12 and 13. This separation is also consistent with the definitions in ref 22, but it should be kept in mind that the contact and pseudocontact terms in eqs 10 and 11 keep their traditional meaning only approximately.¹⁹ For example, the contact shift in eq 12 is not defined exclusively by the spin density at the nucleus, because in the relativistic theory the spin–dipolar and paramagnetic spin–orbit operators also give isotropic contributions to the HFC tensor. Similarly, the pseudocontact shift does not contain structural information in

the form as anticipated in ref 4, because, for example, the Fermi contact operator have an anisotropic contribution to the HFC tensor.

In the following, we summarize the important aspects of the four-component relativistic calculations of all ingredients in eq 6. For more details about evaluation of the \mathbf{g} , HFC, and chemical shielding tensors at the four-component DFT level, we refer the interested reader to refs 36–38, 40, and 41. First we will discuss the orbital part of the pNMR tensor, followed by a brief summary of the four-component calculations of the \mathbf{g} and HFC tensors.

We begin with the expression for the Dirac–Kohn–Sham energy in the presence of the external magnetic field and the magnetic field due to the magnetic moment of a nucleus. In the framework of the Born–Oppenheimer approximation (using the Hartree system of atomic units throughout this paper) we can write

$$E^{(\vec{B}, \vec{\mu}^M)} = E_{\text{kin}}^{(\vec{B}, \vec{\mu}^M)} + E_{\text{nuc}}^{(\vec{B}, \vec{\mu}^M)} + E_{\text{ee}}^{(\vec{B}, \vec{\mu}^M)} + E_{\text{xc}}^{(\vec{B}, \vec{\mu}^M)} \quad (14)$$

The right-hand side of this equation consists of relativistic kinetic energy, electron–nucleus Coulomb energy, electron–electron Coulomb energy, and exchange–correlation energy functional, respectively. We write the relativistic kinetic energy, in the framework of DFT, as

$$E_{\text{kin}}^{(\vec{B}, \vec{\mu}^M)} = \left\langle \varphi_i^{(\vec{B}, \vec{\mu}^M)} \left| (\beta - \mathbf{1})c^2 + c\vec{\alpha} \cdot \vec{p} + \vec{\alpha} \cdot \vec{A}_{\vec{B}_0} + \vec{\alpha} \cdot \vec{A}_{\vec{\mu}^M} \right| \varphi_i^{(\vec{B}, \vec{\mu}^M)} \right\rangle \quad (15)$$

We have here and in the following assumed implicit summation over repeated indices. In this equation, c is the speed of light, \vec{p} is the momentum operator, φ_i represents the i th four-component molecular orbital (MO), $\vec{A}_{\vec{B}_0}$ is the vector potential generated by the external magnetic field \vec{B} with gauge origin \vec{R}_0 , $\vec{A}_{\vec{\mu}^M}$ denotes the vector potential generated by the magnetic moment of nucleus $\vec{\mu}^M$, and the four-by-four matrices β and $\vec{\alpha}$ have the usual two-by-two representation:

$$\beta \equiv \begin{pmatrix} 1 & 0 \\ 0 & -1 \end{pmatrix} \quad \vec{\alpha} \equiv \begin{pmatrix} 0 & \vec{\sigma} \\ \vec{\sigma} & 0 \end{pmatrix} \quad (16)$$

where $\vec{\sigma}$ are the Pauli matrices. Superscripts $(\vec{B}, \vec{\mu}^M)$ denote the dependence of the quantities on the applied perturbations. It is useful to decompose the four-component MOs in eq 15 into large (L) and small (S) component parts:

$$\varphi_i^{(\vec{B}, \vec{\mu}^M)} = \begin{pmatrix} \varphi_i^{\text{L}(\vec{B}, \vec{\mu}^M)} \\ \varphi_i^{\text{S}(\vec{B}, \vec{\mu}^M)} \end{pmatrix} \quad (17)$$

We can furthermore express the large and small components of the four-component MOs as linear combinations of basis functions χ_λ^{L} and χ_λ^{S} :

$$\varphi_i^{\text{L}(\vec{B}, \vec{\mu}^M)} = C_{\lambda i}^{\text{L}(\vec{B}, \vec{\mu}^M)} \chi_\lambda^{\text{L}(\vec{B}, \vec{\mu}^M)} \quad (18)$$

$$\varphi_i^{\text{S}(\vec{B}, \vec{\mu}^M)} = C_{\lambda i}^{\text{S}(\vec{B}, \vec{\mu}^M)} \chi_\lambda^{\text{S}(\vec{B}, \vec{\mu}^M)} \quad (19)$$

We will refer to \mathbf{C}^{L} and \mathbf{C}^{S} as MO coefficients for the large and small components, respectively. For more details we refer to ref 40.

The coupling mediated by the operator $\vec{\alpha}$ in eq 15 is the source of serious numerical problems.⁴⁷ However, in the

absence of magnetic fields it is possible to avoid them by using a restricted kinetically balanced basis set (RKB) for the small component.^{47,48}

$$\chi_\lambda^{\text{L}(0,0)} \equiv \chi_\lambda \quad (20)$$

$$\chi_\lambda^{\text{S}(0,0)} \equiv \frac{1}{2c} \vec{\sigma} \cdot \vec{p} \chi_\lambda \quad (21)$$

where χ_λ denotes the λ th atomic orbital (AO) centered on a nucleus at \vec{R}_λ .

Although the RKB basis in the absence of magnetic fields has been shown to be an excellent solution to the numerical problems, in the presence of magnetic fields it leads to very poor basis-set convergence even for rare-gas chemical shieldings.⁴⁹ A very efficient solution to this problem is to use restricted magnetically balanced (RMB) basis sets^{40,41,43} (for alternative methods, see refs 50 and 51). To get even faster basis-set convergence in the presence of the external magnetic field, one should combine the RMB basis with the well-known London atomic orbitals:^{41,52,53}

$$\chi_\lambda^{\text{L}(\vec{B}, \vec{\mu}^M)} \equiv \omega_\lambda^{(\vec{B})} \chi_\lambda \quad (22)$$

$$\chi_\lambda^{\text{S}(\vec{B}, \vec{\mu}^M)} \equiv \frac{1}{2c} \omega_\lambda^{(\vec{B})} \left(\vec{\sigma} \cdot \vec{p} + \frac{1}{c} \vec{\sigma} \cdot \vec{A}_{\vec{B}_\lambda} + \frac{1}{c} \vec{\sigma} \cdot \vec{A}_{\vec{\mu}^M} \right) \chi_\lambda \quad (23)$$

where the gauge of the vector potential $\vec{A}_{\vec{B}_\lambda}$ is at the center of the atomic orbital χ_λ and the London phase factor $\omega_\lambda^{(\vec{B})}$ is given by

$$\omega_\lambda^{(\vec{B})} \equiv \exp \left\{ -\frac{i}{2c} [\vec{B} \times (\vec{R}_\lambda - \vec{R}_0)] \cdot \vec{r} \right\} \quad (24)$$

The phase factor $\omega_\lambda^{(\vec{B})}$ shifts the global gauge origin \vec{R}_0 to the natural gauge of the λ th atomic orbital \vec{R}_λ ,⁵⁴ chosen to be the position of the nucleus to which the orbital is attached.

By considering eqs 17, 22, and 23, we note that the magnetic response of the four-component MO can be decomposed into regular, magnetic, and London parts:

$$\varphi_i^{(1,0)_u} = \varphi_i^{\text{r}(1,0)_u} + \varphi_i^{\text{m}(1,0)_u} + \varphi_i^{\text{o}(1,0)_u} \quad (25)$$

where $(1,0)_u$ and $(0,1)_v^{\text{M}}$ denote derivatives with respect to B_u and μ_v^{M} , respectively. The different contributions in eq 25 represent derivatives with respect to different parts of the MOs in eq 17. The regular contribution arises from the response of the MO coefficients, the magnetic part originates from the magnetic balance with respect to the external magnetic field (second term in parentheses in eq 23), and the London contribution arises from the phase factor in eqs 22 and 23.

As already discussed, the orbital part of the pNMR tensor for the doublet system (eq 6) can be expressed as the usual NMR shielding tensor for a diamagnetic system:

$$(\sigma_{\text{M}}^{\text{orb}})_{uv} = \frac{\partial^2 E(\vec{B}, \vec{\mu}^M)}{\partial B_u \partial \mu_v^{\text{M}}} \bigg|_{\vec{B}=\vec{\mu}^M=0} \quad (26)$$

The bilinear derivative of the energy can be expressed as follows (see appendix A in ref 40):

$$(\sigma_{\text{M}}^{\text{orb}})_{uv} = \left\langle \varphi_i^{(1,0)_u} \right| D^{(0,1)_v^{\text{M}}} \left| \varphi_i^{(0,0)} \right\rangle + \left\langle \varphi_i^{(0,0)} \right| D^{(0,1)_v^{\text{M}}} \left| \varphi_i^{(1,0)_u} \right\rangle \quad (27)$$

where

$$D^{(0,1)}_v \equiv \frac{\partial}{\partial \mu_v^M} (\vec{\alpha} \cdot \vec{A}_{\vec{\mu}^M}) \quad (28)$$

We note that in relativistic theory (in contrast to non-relativistic theory) there is no term expressed as an expectation value of a bilinear operator over unperturbed MOs (the so-called diamagnetic term) in the MO representation. However, if we switch to the AO representation, the missing diamagnetic term will arise from the magnetic part of the response of MO, $\varphi_i^{m(1,0)}_v$:

$$(\sigma_M^{\text{orb}})_{uv}^D \equiv \left\langle \varphi_i^{m(1,0)}_v \left| D^{(0,1)}_v \right| \varphi_i^{(0,0)} \right\rangle + \left\langle \varphi_i^{(0,0)} \left| D^{(0,1)}_v \right| \varphi_i^{m(1,0)}_v \right\rangle \quad (29)$$

This is an intrinsic feature of an explicitly magnetically balanced basis such as the one defined in eq 23. Without the magnetic balance, the diamagnetic contribution is “hidden” in the formally paramagnetic term, in particular in the part that involves the summation over negative-energy states.⁵⁵ Consequently, for reproducing correctly the diamagnetic contribution, a very large basis set is required. Clearly, the use of a magnetically balanced basis is preferable since it allows one to significantly reduce the computational effort.

The usual paramagnetic contributions can be obtained from the regular and London parts of the response MO (eq 25). For a detailed derivation of the working equations, see refs 40 and 41.

Calculation of the orbital contribution at the four-component level was performed according to the procedure for calculations of other properties of open-shell systems (such as the HFC tensor, **g** tensor, and ZFS), that is, by use of three self-consistent field (SCF) procedures, one for each of the principal axes of the **g** tensor.^{36–38,56}

We will employ the following definition of the **g** and HFC tensors for an effective doublet system:

$$g_{ut} = 4c \frac{\partial E(\vec{B}, J_t)}{\partial B_u} \bigg|_{\vec{B}=0} \quad (30)$$

$$(A_M)_{vt} = 2 \frac{\partial E(\vec{I}^M, J_t)}{\partial I_v^M} \bigg|_{\vec{I}^M=0} \quad (31)$$

where \vec{I}^M is the nuclear spin and \vec{J} represents the total magnetization vector. From eqs 30 and 31 it is clear that, in the four-component relativistic domain, the **g** and HFC tensors are first-order properties. Using the Hellman–Feynman theorem in the x representation,^{57,58} we can write

$$g_{ut} = 4c \left\langle \varphi_i^{(0,J_t)} \left| \frac{\partial}{\partial B_u} (\vec{\alpha} \cdot \vec{A}_{\vec{B}_0}) \right| \varphi_i^{(0,J_t)} \right\rangle \quad (32)$$

$$(A_M)_{vt} = 2 \left\langle \varphi_i^{(0,J_t)} \left| \frac{\partial}{\partial I_v^M} (\vec{\alpha} \cdot \vec{A}_{\vec{\mu}^M}) \right| \varphi_i^{(0,J_t)} \right\rangle \quad (33)$$

Note that because the MOs in the above expressions do not depend on the magnetic fields, it is sufficient to use the RKB basis (eqs 20 and 21). For more details on the four-component calculation of the **g** and HFC tensors, see refs 37 and 38.

3. COMPUTATIONAL DETAILS

All calculations have been carried out at the four-component matrix Dirac–Kohn–Sham (mDKS) level of theory with the ReSPECT program package (version 3.3.0).⁵⁹ A noncollinear Kramers-unrestricted formulation of the BP86 functional^{60–62} was used to account for exchange and correlation effects. We have chosen the BP86 functional to remain consistent with previous work by Rastrelli and Bagno.³² Dyall’s all-electron uncontracted basis sets of valence double- ζ (21s 14p 10d 2f), triple- ζ (28s 20p 13d 4f 2g), and quadruple- ζ (33s 25p 17d 5f 4g 2h) quality were used for the ruthenium atom.⁶³ For the light elements, we employed the uncontracted pcJ-X ($X = 1, 2, 3$) basis sets of Jensen.⁶⁴ Unless otherwise stated, we present the results obtained with the valence triple- ζ basis sets. The molecular structures have been taken from ref 32.

Integration of the exchange–correlation parts was done numerically on a molecular grid of ultrafine quality with an adaptive size in the angular part combined with a fixed number of radial quadrature grid points: H (50), second-row elements (60), third-row elements (70), and Ru (90). The exchange–correlation potential was calculated analytically by means of an automatic differentiation technique, as implemented in the XCFun library.⁶⁵ First derivatives of the BP86 exchange–correlation potential (kernel) were evaluated for closed-shell systems analytically, whereas for open-shell systems a finite difference method (with a step length of 10^{-3}) was used.⁶⁶ In order to improve the convergence of the coupled-perturbed equations, we evaluated the XC kernel using only a local SVWNS⁶⁷ potential (ALDA approach). The error that arises from the use of the ALDA approximation was estimated from closed-shell analogues of the Ru complexes and did not exceed 0.5 ppm for NAMI and 1.1 ppm for *mer*-Ru(ma)₃.

All relativistic SCF calculations were done with a finite-size nucleus model employing a Gaussian charge distribution, whereas for the chemical shielding and hyperfine coupling tensors, the point model for nuclear charge and magnetic moment distributions was assumed. The nuclear magnetic moment of ¹H was taken to be 2.792 847 34 μ_N .⁶⁸ The computed nuclear shieldings were converted to chemical shifts [δ , in parts per million (ppm)] relative to the shielding of tetramethylsilane, TMS (calculated four-component value for TMS = 30.87 ppm), and all temperature-dependent NMR signals were evaluated for experimental temperatures.

Finally, we highlight two important points: First, all calculations of the NMR shielding tensors were performed without any accelerating techniques, such as the density fitting approach used in our previous studies,⁴² and all results are therefore free of errors that arise from using auxiliary basis sets. Second, the present implementation of the **g** tensor does not include London atomic orbitals (LAO) and the results are therefore not fully gauge invariant. We performed several test calculations on the NAMI molecule in order to estimate the error introduced by using a common gauge origin (CGO) approximation in the calculation of **g** tensors. The components of the **g** tensor varied by less than 0.1% when the gauge origin was moved from the center of mass to different atomic centers.

4. RESULTS AND DISCUSSION

We will here discuss the results obtained with our new approach for two Ru(III) complexes (see structures in Figure 1). These systems were chosen because the results of relativistic ZORA calculations (by Rastrelli and Bagno³²) and reliable

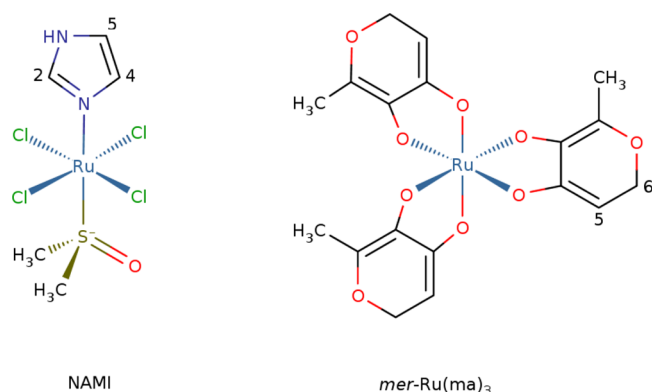


Figure 1. Structures and numbering of investigated Ru(III) systems.

experimental data [*mer*-Ru(ma)₃]⁴⁴ and a new anti-tumor metastasis inhibitor (NAMI)⁴⁵ are available for both complexes.

NAMI. Our results, together with the results of Rastrelli and Bagno³² and available experimental data, are collected in Table 1. For the theoretical results, individual contributions to the isotropic pNMR shielding constants are also reported. From these data (graphically presented in Figure 2), we note that all theoretical methods systematically overestimate the experimental results, although the four-component method performs best.

Table 1. Calculated and Experimental ¹H pNMR Isotropic Shieldings of NAMI^a

method ^b	A_{iso}	$\sigma_{\text{iso}}^{\text{orb}}$	$\sigma_{\text{iso}}^{\text{fc}}$	$\sigma_{\text{iso}}^{\text{pc}}$	σ_{iso}	δ_{iso}
Proton Label CH ₃						
NR	−0.17	33.41	5.39		38.80	−7.4
ZORA	−0.32	27.78	9.41		37.18	−5.8
mDKS	−0.28	32.83	7.98	2.15	42.96	−12.1
exptl						−14.5
Proton Label H-2						
NR	0.23	25.87	−7.28		18.59	12.9
ZORA	0.09	22.66	−2.73		19.93	11.4
mDKS	0.23	25.80	−6.42	3.45	22.82	8.0
exptl						−5.6
Proton Label H-4						
NR	−0.06	26.22	1.91		28.13	3.3
ZORA	−0.11	22.53	3.21		25.73	5.6
mDKS	−0.15	26.03	4.31	3.19	33.53	−2.7
exptl						−7.8
Proton Label H-5						
NR	−0.10	27.61	3.11		30.72	0.7
ZORA	−0.15	25.09	4.29		29.38	2.0
mDKS	−0.17	27.51	4.72	1.34	33.57	−2.7
exptl						−3.5
Proton Label NH						
NR	−0.00	24.55	0.00		24.56	6.9
ZORA	−0.07	23.44	2.11		25.54	5.8
mDKS	−0.04	24.80	1.25	1.28	27.33	3.5
exptl						

^aIn all calculations the BP86 functional was employed. HFC constants A_{iso} are in megahertz. Isotropic shieldings are in parts per million (ppm). ^bNR (nonrelativistic) and ZORA (zero-order regular approximation), data taken from ref 32; mDKS (four-component matrix Dirac–Kohn–Sham level of theory), this work; exptl, experimental data taken from ref 45 ($T = 25\text{ }^{\circ}\text{C}$).

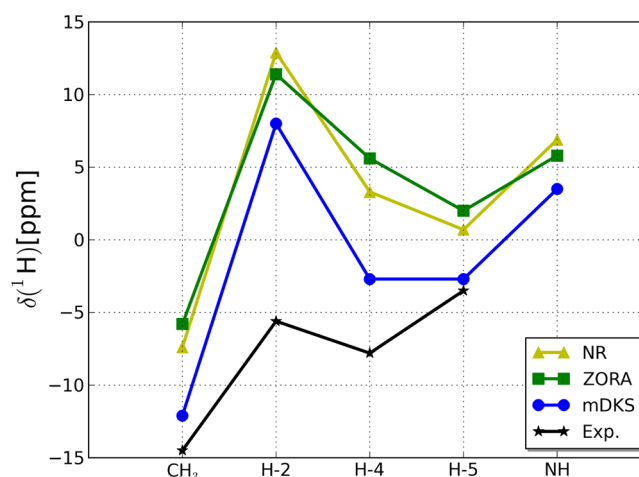


Figure 2. Calculated and experimental ¹H pNMR isotropic shifts of NAMI (for explanation of the legend, see Table 1).

To analyze the effect of basis-set quality on the results, additional calculations with different basis sets were performed. These results are collected in Table 2. Table 2 reveals fast basis-

Table 2. Basis-Set Convergence of ¹H pNMR Isotropic Shifts Calculated by mDKS Method for NAMI^a

basis-set quality	CH ₃	H-2	H-4	H-5	NH
double- ζ	−12.0	7.3	−3.6	−3.0	3.1
triple- ζ	−12.1	8.0	−2.7	−2.7	3.5
quadruple- ζ	−12.0	7.8	−2.7	−2.5	4.4

^aIsotropic shifts are in parts per million (ppm).

set convergence for our approach. Even the double- ζ basis set gives reliable results when the range of the proton shielding scale is considered. To be on the safe side, we have chosen to use the triple- ζ quality basis set for the rest of our calculations. One of the possible reasons for the discrepancy of theoretical and experimental results may be the neglect of vibrational corrections and/or effects of the solvent in our theoretical calculations. To shed some light on this topic, we have performed calculations with modified geometries for NAMI. In one series of calculations, we investigated the effect of stretching the Ru–N bond (see Figure 3). The overall agreement with experiment as well as the trend in the calculated results was improved when enlarging the Ru–N distance. More importantly, all calculations displayed a larger effect of geometry changes on the H-2 proton shielding than on the rest of the protons in the system. Since the shift on this proton has the poorest agreement with experiment, this confirms our hypothesis that vibrational and solvent effects need to be taken into account in order to fully reproduce the experimental data. Rotating the imidazole group around the Ru–N bond confirmed this trend, although the overall changes in the pNMR shifts were smaller than in the case of stretching of the Ru–N bond (the H-2 pNMR shielding varied between 7.5 and 10.9 ppm).

Analysis of the different contributions to the pNMR shift calculated at the four-component level (see Table 1) suggests that the pseudocontact term should not be neglected, in particular for protons closer to the metal center (H-2 and H-4). Autschbach et al.³³ calculated the pseudocontact shift using the ZORA Hamiltonian (with the PBE functional and a slightly

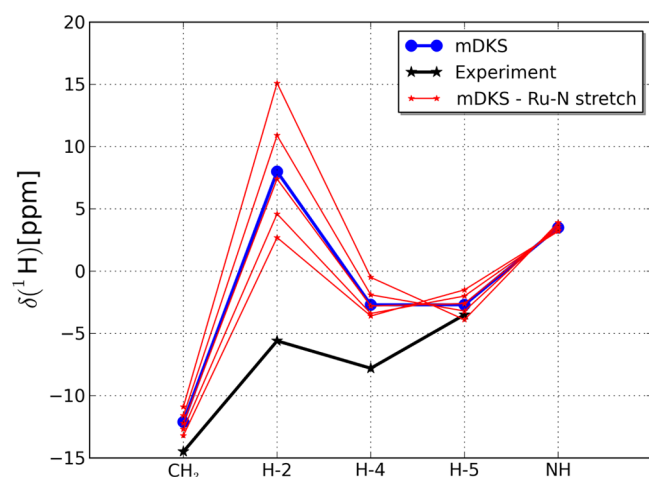


Figure 3. Effect of stretching of Ru–N bond (in the interval 1.9–2.3 Å) on ^1H pNMR isotropic shifts of NAMI compound. Closer to the experimental data are results with longer bonds. mDKS, results with unchanged geometry (Ru–N 2.0813 Å); experiment, results from ref 45.

different definition of $\delta_{\text{M}}^{\text{cc}}$, obtaining qualitatively similar results as ours with the full relativistic Hamiltonian (CH₃, 1.41 ppm; H-2, 2.09 ppm; H-4, 2.30 ppm; H-5, 0.98 ppm; and NH, 0.99 ppm).

There are surprisingly large differences between the ZORA and mDKS results for orbital and contact terms. The orbital contributions obtained with ZORA are systematically underestimated compared to their four-component counterparts. Figure 4 reveals that even the nonrelativistic data better agree

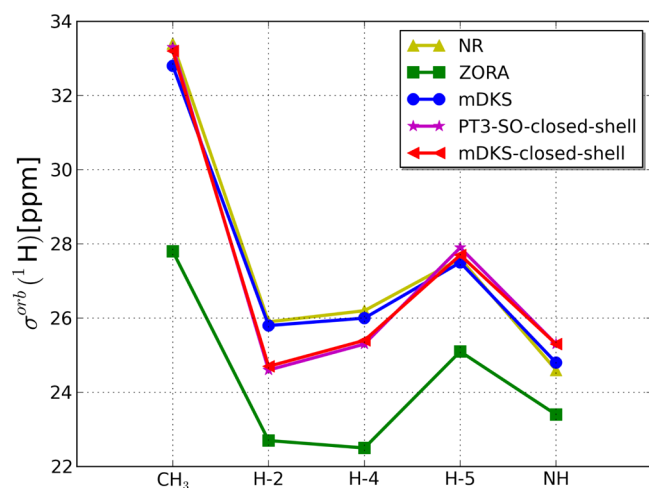


Figure 4. Orbital contribution to ^1H pNMR isotropic shifts of NAMI compound. NR and ZORA: Data taken from ref 32. mDKS: Four-component open-shell calculations. PT3-SO-closed-shell: Third-order perturbation theory²⁵ calculations of closed-shell analogue of NAMI compound. mDKS-closed-shell: Four-component calculations of closed-shell analogue of NAMI compound using BP86 potential and kernel to match PT3-SO calculations.

with the four-component results for the orbital term than those obtained with ZORA. This suggests that, for the complexes considered, the relativistic effects for the orbital term are negligible. This was independently confirmed by a comparison of the mDKS results with data obtained by use of third-order perturbation theory²⁵ for the Ru(II) complex (the closed-shell

analogue of NAMI), where the biggest SO correction was only 0.5 ppm for the H-2 proton. The largest difference in the contact terms between the two relativistic approaches (ZORA and mDKS) is for proton H-2. A closer analysis of the four-component results for the HFC constants shows that the PSO operator contributes 3.1 ppm to the total value of −6.42 ppm (thus partially canceling the rest of the contributions). Because the PSO contribution for protons arises to a great extent from SO effects, it is clear that, in order to obtain the correct values, a proper treatment of both relativistic and spin-polarization effects is mandatory.

mer-Ru(ma)₃. In Table 3 we have collected the theoretical and experimental data. Also shown here are different contributions to calculated values of the pNMR shieldings. The data presented in Table 3 exhibit very small differences [except for the CH₃(a) and CH₃(b) groups] between the results of the two relativistic methods (mDKS and ZORA). This outcome could be expected, as all protons are rather far away from the metal center and thus SO relativistic effects can be expected to be small. Since the H-5 and H-6 protons are positioned in the plane of the rings, they are less affected by spin polarization going very effectively via the extended π -electron system. This requires additional spin-polarization of the σ orbitals by the π -orbitals in order to contribute significantly to the contact shift on those protons. However, spin-polarization of the π -electron system has a nonzero effect on protons of the CH₃ groups, giving rise to the larger values observed for CH₃(a) and CH₃(b) [according to Rastrelli and Bagno,³² the very small values for contact contribution to the CH₃(c) proton are caused by “the distorted coordination geometry of the maltolato moieties”]. This can be nicely seen from the analysis of hyperfine coupling constants (HFCC) for individual protons in the CH₃ groups. The HFCC are much smaller for the (approximately) in-plane hydrogens [0.26 MHz for in-plane versus 2.29 and 3.69 MHz for out-of-plane hydrogens in the CH₃(a) group and 0.15 MHz for in-plane versus 3.59 and 4.42 MHz for out-of-plane hydrogens in the CH₃(b) group]. When the CH₃(c) group was rotated to have one hydrogen in-plane, the corresponding HFCC show the same trend (0.06 MHz for the in-plane hydrogen versus 0.50 and −0.43 MHz for the out-of-plane hydrogens) as in the groups a and b but on a smaller scale. The only noticeable difference between the mDKS and ZORA results is in the contact term for CH₃(a) and CH₃(b) groups. Most likely this is a consequence of using less flexible basis sets in the ZORA calculations. Autschbach et al.³³ observed similar relative differences for HFC constants when the JCPL basis set was used instead of TZ2P. This confirms the well-known sensitivity of HFC constants to basis-set quality and exchange–correlation functionals employed as well as the general numerical stability of the code. Thus one must take special care in choosing a basis set that would ensure practical convergence of the results with respect to basis-set quality. The values obtained for the pseudoccontact term are small and have negligible effect on the results. This can also be due to the large distance between the metal center and the protons.

In Table 4 the calculated g tensors for the NAMI and mer-Ru(ma)₃ compounds are presented. For NAMI, the non-relativistic calculations⁶⁹ significantly overestimate the g tensor in comparison with our four-component calculations, whereas for mer-Ru(ma)₃, both approaches give similar results. The ZORA results differ significantly from the fully relativistic mDKS data for both compounds. Since we intentionally used

Table 3. Calculated and Experimental ^1H pNMR Isotropic Shieldings of $\text{mer-Ru}(\text{ma})_3^a$

method ^b	A_{iso}	$\sigma_{\text{iso}}^{\text{orb}}$	$\sigma_{\text{iso}}^{\text{fc}}$	$\sigma_{\text{iso}}^{\text{pc}}$	σ_{iso}	δ_{iso}
Proton Label CH ₃ (a)						
NR	2.38	28.59	−69.03		−40.44	71.89
ZORA	2.53	29.64	−69.59		−39.95	71.3
mDKS	2.08	28.78	−56.39	−1.27	−28.87	59.74
exptl						41.03
Proton Label CH ₃ (b)						
NR	3.08	28.71	−89.47		−60.76	92.21
ZORA	3.27	29.65	−90.20		−60.55	91.9
mDKS	2.72	29.42	−73.80	−0.32	−44.70	75.57
exptl						43.17
Proton Label CH ₃ (c)						
NR	−0.25	28.76	7.14		35.90	−4.45
ZORA	−0.29	29.28	8.05		37.34	−6.0
mDKS	−0.31	28.67	8.46	−1.11	36.01	−5.15
exptl						21.11
Proton Label H-5a						
NR	−0.16	24.94	4.70		29.63	1.82
ZORA	−0.27	25.71	7.46		33.18	−1.8
mDKS	−0.28	25.04	7.53	1.33	33.90	−3.03
exptl						−0.87
Proton Label H-6a						
NR	−0.41	23.85	11.81		35.66	−4.21
ZORA	−0.35	25.18	9.53		34.71	−3.4
mDKS	−0.29	24.13	7.94	0.36	32.44	−1.57
exptl						0.92
Proton Label H-5b						
NR	−0.41	24.84	11.97		36.81	−5.36
ZORA	−0.58	25.74	16.04		41.78	−10.4
mDKS	−0.54	24.78	14.70	1.35	40.83	−9.96
exptl						−4.61
Proton Label H-6b						
NR	0.03	23.83	−0.94		22.89	8.56
ZORA	0.24	25.38	−6.71		18.67	12.7
mDKS	0.26	24.36	−7.03	0.44	17.77	13.10
exptl						3.43
Proton Label H-5c						
NR	0.37	24.74	−10.88		13.86	17.59
ZORA	0.38	25.30	−10.38		14.92	16.4
mDKS	0.38	23.72	−10.21	−0.48	13.03	17.84
exptl						11.84
Proton Label H-6c						
NR	0.01	23.92	−0.30		23.62	7.83
ZORA	0.07	24.74	−1.99		22.75	8.6
mDKS	0.10	23.32	−2.63	−0.36	20.33	10.54
exptl						9.20

^aIn all calculations the BP86 functional was employed. HFC constants A_{iso} are in megahertz. Isotropic shieldings are in parts per million (ppm). ^bNR (nonrelativistic) and ZORA (zero-order regular approximation), data taken from ref 32; mDKS (four-component matrix Dirac–Kohn–Sham level of theory), this work; exptl, experimental data taken from ref 44 ($T = 22\text{ }^\circ\text{C}$).

the same functional and geometry for the compounds as in the ZORA calculations, this discrepancy indicates shortcomings in the ZORA two-component approach in comparison to the four-component method, already for 4d element compounds.

Whereas there are several aspects of accuracy of the calculations presented here that might be improved in future studies (such as taking a better DFT functional or modeling solvent effects), we still believe we can address an important

Table 4. Isotropic g Tensors for NAMI and $\text{mer-Ru}(\text{ma})_3$

method ^a	NAMI	$\text{mer-Ru}(\text{ma})_3$
NR	2.345	2.172
ZORA	2.194	2.081
mDKS	2.035	2.160

^aNR (nonrelativistic) and ZORA (zero-order regular approximation), data taken from ref 32; mDKS (four-component matrix Dirac–Kohn–Sham level of theory), this work.

point affecting the comparison between theoretical results and experimental data. How reliable are the experimental assignments? Can a better agreement with the theoretical data be achieved by reassigning some of the experimental shielding constants? In the experimental pNMR study of Kennedy et al.,⁴⁴ a coupling between protons H-5 and H-6 was observed, and therefore their relative assignment is fixed. However, the assignment of pairs of protons to the different ligands is more problematic. If it is assumed that we can reassign some of the experimental data (switching protons 5 and 6 between groups a and c, in contrast to the assignment of Rastrelli and Bagno,³² see Table 3), a comparison of the left (original assignment) and right plots (our assignment) in Figure 5 suggests that reassignment may be in order. However, in order to make a definite conclusion, a wider variety of DFT functionals must be tested.

There are apparent discrepancies between the experimental and calculated pNMR shifts of the CH₃ groups. Rastrelli and Bagno³² attributed this to inaccuracies in the optimized geometry. Because we have employed the same geometries in our calculations, it is interesting to see to what extent a possible inaccuracy in the geometries might affect the resulting shifts. To check the geometry dependence of the results, we have performed calculations with rotated CH₃ groups and modified distances of the Ru–O bonds compared to the X-ray structure available in ref 44. These changes in the geometry have only a negligible effect on the proton shifts studied. We believe that the most probable reason for the discrepancy between our results and experiment is the limitation of DFT itself. The use of a better functional might improve the situation. Also, since the measurements were done in solution (CD₂Cl₂), solvent effects should be taken into account for a more reliable model.

It is worth noting that the calculated peaks of the CH₃(a) and CH₃(b) groups lie outside the experimental range. This indicates that the reported experimental shifts of the CH₃(a) and CH₃(b) groups might be misassigned and have a different origin [i.e., the peaks might arise from contaminants and not from $\text{mer-Ru}(\text{ma})_3$]. Confirming these speculations would, however, require a more detailed analysis of the experimental procedures and additional calculations. We have not pursued this issue any further since it is beyond the scope of this work.

5. CONCLUSIONS

A four-component relativistic DFT theory for the calculation of NMR shielding tensors of paramagnetic doublet substances has been presented. The new method automatically includes all relativistic effects described by the Dirac–Coulomb Hamiltonian. The method has been implemented in the ReSPECT program package,⁵⁹ taking advantage of the existing efficient implementations of EPR and NMR parameters. This allows us to apply the method to chemically interesting systems while at the same time retaining the high accuracy of the four-

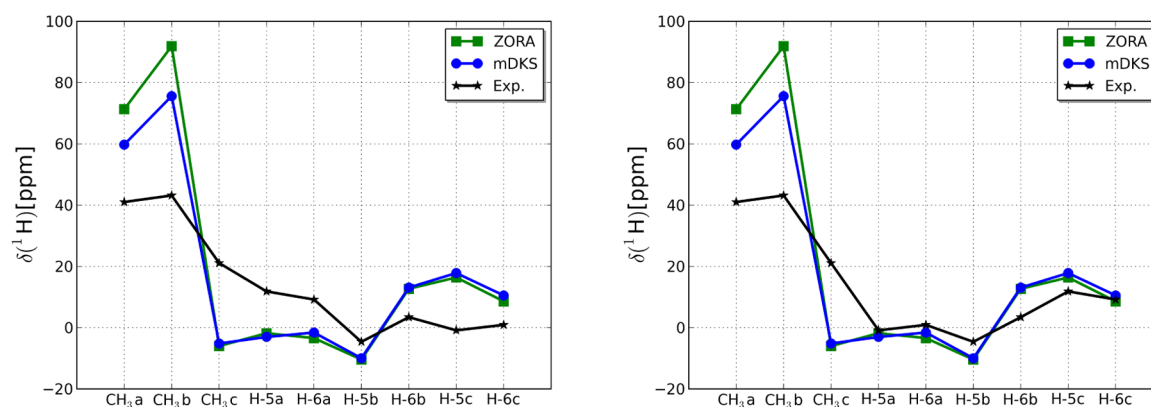


Figure 5. Calculated and experimental ^1H pNMR isotropic shifts of *mer*-Ru(ma) $_3$. (Left) Original assignment taken from ref 32. (Right) Experimental data are assigned to better match the mDKS calculation (within experimental constraints). For explanation of the legend see Table 3

component relativistic theory, thus avoiding most of the approximations employed in earlier theoretical studies.

A separation into contact and pseudocontact terms within relativistic theory for pNMR shieldings was proposed (eqs 10 and 11). The relativistic insight into pseudocontact and contact terms revealed that their nature is more complicated than it is assumed by commonly used simplified models (see also ref 19). Extraction of the value of spin density at the position of an investigated nucleus is even more problematic: at the two- or four-component relativistic level of theory, the Fermi contact contribution to the hyperfine coupling constant is not defined solely by the spin density. This means that the development of more accurate relativistic methods for the calculation of pNMR shieldings must be accompanied by development of new interpretation tools for analysis of the results obtained and more advanced models for interpretation of experimental results.

All calculated pNMR shifts are in good qualitative agreement with experimental data, and the observed deviation from experiment for the NAMI complex can be attributed to the sensitivity of the pNMR results to changes in geometry. Therefore, the inclusion of vibrational and/or solvent effects is necessary. The results for *mer*-Ru(ma) $_3$ demonstrate the usefulness of quantum-chemical methods in helping to assign experimentally measured data.

We disagree with Rastrelli and Bagno³² in their conclusion that relativistic calculations for Ru(III) complexes are not required. Although only the ^1H pNMR shifts were investigated here, we found noticeable differences between the four-component results and those obtained with more approximate schemes. In the case of NAMI, the orbital contribution to the shielding obtained with the ZORA Hamiltonian systematically undershot our four-component data. Sizable differences were observed for some of the calculated hyperfine coupling constants, which is not surprising when it is considered that the HFC tensor is a very sensitive property requiring an accurate treatment of relativistic and spin-polarization effects even for nuclei as light as hydrogen.

We finally note that an important limitation of the method presented here is the restriction that it can only be used for systems without ZFS. Extension of the approach to systems with higher degeneracies and non-negligible ZFS is currently being developed in our group.

AUTHOR INFORMATION

Corresponding Author

*E-mail stanislav.komorovsky@uit.no.

Notes

The authors declare no competing financial interest.

ACKNOWLEDGMENTS

We are grateful to Professor Alessandro Bagno for providing us geometries of the compounds studied. This work was supported by the Research Council of Norway through a Center of Excellence grant (179568/V30) and through a research grant (214095-F20). A computational grant from the Norwegian Supercomputing Program (nn4654K) is also gratefully acknowledged. Furthermore, we acknowledge EU financial support within the Marie Curie Initial Training Networks action (FP7-PEOPLE-2012-ITN), project 317127 “pNMR”, and Slovak grant agencies VEGA (grant 2/0148/13) and APVV (grant APVV-0483-10) for their financial support.

REFERENCES

- (1) *Encyclopedia of NMR*; Harris, R. K., Wasylishen, R. E., Eds.; J. Wiley & Sons: Chichester, U.K., 2012.
- (2) *Handbook of Magnetism and Advanced Magnetic Materials*; Kronmüller, H., Parkin, S., Eds.; J. Wiley & Sons: Chichester, U.K., 2007.
- (3) Kaupp, M.; Köhler, F. H. Combining NMR Spectroscopy and Quantum Chemistry as Tools to Quantify Spin Density Distributions in Molecular Magnetic Compounds. *Coord. Chem. Rev.* **2009**, *253*, 2376–2386.
- (4) Bertini, I.; Luchinat, C.; Parigi, G. Magnetic Susceptibility in Paramagnetic NMR. *Prog. Nucl. Magn. Reson. Spectrosc.* **2002**, *40*, 249–273.
- (5) Bertini, I.; Luchinat, C.; Aime, S. NMR of Paramagnetic Substances. *Coord. Chem. Rev.* **1996**, *150*, R7+.
- (6) Pintacuda, G.; Kervin, G. Paramagnetic Solid-State Magic-Angle Spinning NMR Spectroscopy. In *Modern NMR Methodology*; Heise, H., Matthews, S., Eds.; Springer-Verlag: Berlin, 2013; Vol. 335, pp 157–200.
- (7) Kurland, R. J.; McGarvey, B. R. Isotropic NMR Shifts in Transition Metal Complexes: The Calculation of the Fermi Contact and Pseudocontact Terms. *J. Magn. Reson.* **1970**, *2*, 286–301.
- (8) Ramsey, N. F. Magnetic Shielding of Nuclei in Molecules. *Phys. Rev.* **1950**, *78*, 699–703.
- (9) Ramsey, N. F. Dependence of Magnetic Shielding of Nuclei upon Molecular Orientation. *Phys. Rev.* **1951**, *83*, 540–541.
- (10) Pyykkö, P. Theory of NMR Parameters. From Ramsey to Relativity, 1953 to 1983. In *Calculation of NMR and EPR Parameters*:

Theory and Applications; Kaupp, M., Bühl, M., Malkin, V. G., Eds.; Wiley-VCH: Weinheim, Germany, 2004; Chapt. 2.

(11) McConnell, H. M.; Chesnut, D. B. Theory of Isotropic Hyperfine Interactions in π -electron Radicals. *J. Chem. Phys.* **1958**, *28*, 107–117.

(12) McConnell, H. M.; Robertson, R. E. Isotropic Nuclear Resonance Shifts. *J. Chem. Phys.* **1958**, *29*, 1361–1365.

(13) Rinkevicius, Z.; Vaara, J.; Telyatnyk, L.; Vahtras, O. Calculations of Nuclear Magnetic Shielding in Paramagnetic Molecules. *J. Chem. Phys.* **2003**, *118*, 2550–2561.

(14) Telyatnyk, L.; Vaara, J.; Rinkevicius, Z.; Vahtras, O. Influence of Hydrogen Bonding in the Paramagnetic NMR Shieldings of Nitronylnitroxide Derivative Molecules. *J. Phys. Chem. B* **2004**, *108*, 1197–1206.

(15) Kaupp, M.; Reviakine, R.; Malkina, O. L.; Arbuznikov, A.; Schimmelpfennig, B.; Malkin, V. G. Calculation of Electronic g-Tensors for Transition Metal Complexes Using Hybrid Density Functionals and Atomic Meanfield Spin-Orbit Operators. *J. Comput. Chem.* **2002**, *23*, 794–803.

(16) Moon, S.; Patchkovskii, S. First-Principles Calculations of Paramagnetic NMR Shifts. In *Calculation of NMR and EPR Parameters: Theory and Applications*; Kaupp, M., Bühl, M., Malkin, V. G., Eds.; Wiley-VCH: Weinheim, Germany, 2004; Chapt. 20.

(17) Van Den Heuvel, W.; Soncini, A. NMR Chemical Shift in an Electronic State with Arbitrary Degeneracy. *Phys. Rev. Lett.* **2012**, *109*, No. 073001.

(18) Van Den Heuvel, W.; Soncini, A. NMR Chemical Shift as Analytical Derivative of the Helmholtz Free Energy. *J. Chem. Phys.* **2013**, *138*, No. 054113.

(19) Pennanen, T. O.; Vaara, J. Density-Functional Calculations of Relativistic Spin-Orbit Effects on Nuclear Magnetic Shielding in Paramagnetic Molecules. *J. Chem. Phys.* **2005**, *123*, No. 174102.

(20) Pennanen, T. O.; Vaara, J. Nuclear Magnetic Resonance Chemical Shift in an Arbitrary Electronic Spin State. *Phys. Rev. Lett.* **2008**, *100*, No. 133002.

(21) Liimatainen, H.; Pennanen, T. O.; Vaara, J. ^1H Chemical Shifts in Nonaxial, Paramagnetic Chromium(III) Complexes: Application of Novel pNMR Shift Theory(1). *Can. J. Chem.* **2009**, *87*, 954–964.

(22) Hrobárik, P.; Reviakine, R.; Arbuznikov, A. V.; Malkina, O. L.; Malkin, V. G.; Köhler, F. H.; Kaupp, M. Density Functional Calculations of NMR Shielding Tensors for Paramagnetic Systems with Arbitrary Spin Multiplicity: Validation on 3d Metalloenes. *J. Chem. Phys.* **2007**, *126*, No. 024107.

(23) Dyall, K. G.; Faegri, K., Jr. Perturbation Methods. In *Introduction to Relativistic Quantum Chemistry*; Oxford University Press: New York, 2007; Chapt. 17.

(24) Schimmelpfennig, B., *Atomic Spin-Orbit Mean-Field Integral (AMFI) Program*, Stockholm's Universitet, Stockholm, 1996.

(25) Malkin, V. G.; Malkina, O. L.; Salahub, D. R. Spin-Orbit Correction to NMR Shielding Constants from Density Functional Theory. *Chem. Phys. Lett.* **1996**, *261*, 335–345.

(26) Malkina, O. L.; Schimmelpfennig, B.; Kaupp, M.; Hess, B. A.; Chandra, P.; Wahlgren, U.; Malkin, V. G. Spin-Orbit Corrections to NMR Shielding Constants from Density Functional Theory. How Important are the Two-Electron Terms? *Chem. Phys. Lett.* **1998**, *296*, 93–104.

(27) Vaara, J.; Malkina, O. L.; Stoll, H.; Malkin, V. G.; Kaupp, M. Study of Relativistic Effects on Nuclear Shieldings Using Density-Functional Theory and Spin-Orbit Pseudopotentials. *J. Chem. Phys.* **2001**, *114*, 61–71.

(28) Dyall, K. G.; Faegri, K., Jr. Regular Approximations. In *Introduction to Relativistic Quantum Chemistry*; Oxford University Press: New York, 2007; Chapt. 18.

(29) van Lenthe, E.; Ehlers, A.; Baerends, E. J. Geometry Optimizations in the Zero Order Regular Approximation for Relativistic Effects. *J. Chem. Phys.* **1999**, *110*, 8943–8953.

(30) Nichols, P.; Govind, N.; Bylaska, E. J.; De Jong, W. A. Gaussian Basis Set and Planewave Relativistic Spin-Orbit Methods in NWChem. *J. Chem. Theory Comput.* **2009**, *5*, 491–499.

(31) Malkina, O. L.; Vaara, J.; Schimmelpfennig, B.; Munzarová, M.; Malkin, V. G.; Kaupp, M. Density Functional Calculations of Electronic g-Tensors Using Spin-Orbit Pseudopotentials and Mean-Field All-Electron Spin-Orbit Operators. *J. Am. Chem. Soc.* **2000**, *122*, 9206–9218.

(32) Rastrelli, F.; Bagno, A. Predicting the ^1H and ^{13}C NMR Spectra of Paramagnetic Ru(III) Complexes by DFT. *Magn. Reson. Chem.* **2010**, *48*, S132–S141.

(33) Autschbach, J.; Patchkovskii, S.; Pritchard, B. Calculation of Hyperfine Tensors and Paramagnetic NMR Shifts Using the Relativistic Zeroth-Order Regular Approximation and Density Functional Theory. *J. Chem. Theory Comput.* **2011**, *7*, 2175–2188.

(34) Aquino, F.; Pritchard, B.; Autschbach, J. Scalar Relativistic Computations and Localized Orbital Analyses of Nuclear Hyperfine Coupling and Paramagnetic NMR Chemical Shifts. *J. Chem. Theory Comput.* **2012**, *8*, 598–609.

(35) Pritchard, B.; Autschbach, J. Theoretical Investigation of Paramagnetic NMR Shifts in Transition Metal Acetylacetonato Complexes: Analysis of Signs, Magnitudes, and the Role of the Covalency of Ligand-Metal Bonding. *Inorg. Chem.* **2012**, *51*, 8340–8351.

(36) Komorovský, S.; Repiský, M.; Malkina, O. L.; Malkin, V. G.; Malkin, I.; Kaupp, M. Resolution of Identity Dirac-Kohn-Sham Method Using the Large Component Only: Calculations of g-Tensor and Hyperfine Tensor. *J. Chem. Phys.* **2006**, *124*, No. 084108.

(37) Repiský, M.; Komorovský, S.; Malkin, E.; Malkina, O. L.; Malkin, V. G. Relativistic Four-Component Calculations of Electronic g-Tensors in the Matrix Dirac-Kohn-Sham Framework. *Chem. Phys. Lett.* **2010**, *488*, 94–97.

(38) Malkin, E.; Repiský, M.; Komorovský, S.; Mach, P.; Malkina, O. L.; Malkin, V. G. Effects of Finite Size Nuclei in Relativistic Four-Component Calculations of Hyperfine Structure. *J. Chem. Phys.* **2011**, *134*, 044111.

(39) Hrobárik, P.; Repiský, M.; Komorovský, S.; Hrobáriková, V.; Kaupp, M. Assessment of Higher-Order Spin-Orbit Effects on Electronic g-Tensors of d^1 Transition-Metal Complexes by Relativistic Two- and Four-Component Methods. *Theor. Chem. Acc.* **2011**, *129*, 715–725.

(40) Komorovský, S.; Repiský, M.; Malkina, O. L.; Malkin, V. G.; Malkin Ondík, I.; Kaupp, M. A Fully Relativistic Method for Calculation of Nuclear Magnetic Shielding Tensors with a Restricted Magnetically Balanced Basis in the Framework of the Matrix Dirac-Kohn-Sham Equation. *J. Chem. Phys.* **2008**, *128*, 104101.

(41) Komorovský, S.; Repiský, M.; Malkina, O. L.; Malkin, V. G. Fully Relativistic Calculations of NMR Shielding Tensors Using Restricted Magnetically Balanced Basis and Gauge Including Atomic Orbitals. *J. Chem. Phys.* **2010**, *132*, 154101.

(42) Hrobárik, P.; Hrobáriková, V.; Meier, F.; Repiský, M.; Komorovský, S.; Kaupp, M. Relativistic Four-Component DFT Calculations of ^1H NMR Chemical Shifts in Transition-Metal Hydride Complexes: Unusual High-Field Shifts Beyond the Buckingham-Stephens Model. *J. Phys. Chem. A* **2011**, *115*, 5654–5659.

(43) Repiský, M.; Komorovský, S.; Malkina, O. L.; Malkin, V. G. Restricted Magnetically Balanced Basis Applied for Relativistic Calculations of Indirect Nuclear Spin-Spin Coupling Tensors in the Matrix Dirac-Kohn-Sham Framework. *Chem. Phys.* **2009**, *356*, 236–242.

(44) Kennedy, D. C.; Wu, A.; Patrick, B. O.; James, B. R. Tris(pyronato)- and Tris(pyridonato)-Ruthenium(III) Complexes and Solution NMR Studies. *Inorg. Chem.* **2005**, *44*, 6529–6535.

(45) Alessio, E.; Balducci, G.; Lutman, A.; Mestroni, G.; Calligaris, M.; Attia, W. M. Synthesis and Characterization of Two New Classes of Ruthenium(III)-Sulfoxide Complexes with Nitrogen Donor Ligands (L): $\text{Na}[\text{trans-RuCl}_4(\text{R}_2\text{SO})(\text{L})]\dots$ *Inorg. Chim. Acta* **1993**, *203*, 205–217.

(46) Bertini, I.; Luchinat, C.; Parigi, G. Hyperfine Shifts in Low-Spin Iron(III) Hemes: A Ligand Field Analysis. *Eur. J. Inorg. Chem.* **2000**, 2473–2480.

- (47) Stanton, R. E.; Havriliak, S. Kinetic Balance: A Partial Solution to the Problem of Variational Safety in Dirac Calculations. *J. Chem. Phys.* **1984**, *81*, 1910–1918.
- (48) Kutzelnigg, W. Basis Set Expansion of the Dirac Operator without Variational Collapse. *Int. J. Quantum Chem.* **1984**, *25*, 107–129.
- (49) Vaara, J.; Pyykkö, P. Relativistic, Nearly Basis-Set-Limit Nuclear Magnetic Shielding Constants of the Rare Gases He–Rn: A Way to Absolute Nuclear Magnetic Resonance Shielding Scales. *J. Chem. Phys.* **2003**, *118*, 2973–2976.
- (50) Xiao, Y.; Liu, W.; Cheng, L.; Peng, D. Four-Component Relativistic Theory for Nuclear Magnetic Shielding Constants: Critical Assessments of Different Approaches. *J. Chem. Phys.* **2007**, *126*, 214101.
- (51) Olejniczak, M.; Bast, R.; Saue, T.; Pecul, M. A Simple Scheme for Magnetic Balance in Four-Component Relativistic Kohn-Sham Calculations of Nuclear Magnetic Resonance Shielding Constants in a Gaussian Basis. *J. Chem. Phys.* **2012**, *136*, No. 014108.
- (52) London, F. The Quantic Theory of Inter-Atomic Currents in Aromatic Combinations. *J. Phys. Radium* **1937**, *8*, 397–409.
- (53) Cheng, L.; Xiao, Y.; Liu, W. Four-Component Relativistic Theory for Nuclear Magnetic Shielding: Magnetically Balanced Gauge-Including Atomic Orbitals. *J. Chem. Phys.* **2009**, *131*, No. 244113.
- (54) Bak, K. L.; Jørgensen, P.; Helgaker, T.; Ruud, K.; Jensen, H. J. A. Gauge-Origin Independent Multiconfigurational Self-Consistent-Field Theory for Vibrational Circular Dichroism. *J. Chem. Phys.* **1993**, *98*, 8873–8887.
- (55) Aucar, G. A.; Saue, T.; Visscher, L.; Jensen, H. J. A. On the Origin and Contribution of the Diamagnetic Term in Four-Component Relativistic Calculations of Magnetic Properties. *J. Chem. Phys.* **1999**, *110*, 6208–6218.
- (56) Malkin, I.; Malkina, O. L.; Malkin, V. G.; Kaupp, M. Scalar Relativistic Calculations of Hyperfine Coupling Tensors Using the Douglas-Kroll-Hess Method. *Chem. Phys. Lett.* **2004**, *396*, 268–276.
- (57) Hellmann, H. *Einführung in die Quantenchemie*; F. Deuticke: Leipzig, Germany, 1937.
- (58) Feynman, R. P. Forces in Molecules. *Phys. Rev.* **1939**, *56*, 340–343.
- (59) ReSPECT, version 3.3.0, 2013; Relativistic Spectroscopy DFT program of M. Repisky, S. Komorovsky, V. G. Malkin, O. L. Malkina, M. Kaupp, and K. Ruud, with contributions from R. Bast, U. Ekström, S. Knecht, I. Malkin Ondik, and E. Malkin.
- (60) Becke, A. D. Density-Functional Exchange-Energy Approximation with Correct Asymptotic-Behavior. *Phys. Rev. A* **1988**, *38*, 3098–3100.
- (61) Perdew, J. P. Density-Functional Approximation for the Correlation-Energy of the Inhomogeneous Electron-Gas. *Phys. Rev. B* **1986**, *33*, 8822–8824.
- (62) Perdew, J. P. Erratum: Density-Functional Approximation for the Correlation-Energy of the Inhomogeneous Electron-Gas. *Phys. Rev. B* **1986**, *34*, 7406.
- (63) Dyal, K. G. Relativistic Double-Zeta, Triple-Zeta, and Quadruple-Zeta Basis Sets for the 4d Elements Y–Cd. *Theor. Chem. Acc.* **2007**, *117*, 483–489.
- (64) Jensen, F. The Basis Set Convergence of Spin-Spin Coupling Constants Calculated by Density Functional Methods. *J. Chem. Theory Comput.* **2006**, *2*, 1360–1369.
- (65) Ekström, U.; Visscher, L.; Bast, R.; Thorvaldsen, A. J.; Ruud, K. Arbitrary-Order Density Functional Response Theory from Automatic Differentiation. *J. Chem. Theory Comput.* **2010**, *6*, 1971–1980.
- (66) After calculation of the exchange–correlation potential in AO representation for electron density $\rho_0(\pm\lambda)$ and spin densities $\rho_i(\pm\lambda)$, where $\rho_0(\pm\lambda) = \rho_0^{(0,0)} \pm \lambda\rho_0^{(1,0)}$ and $\rho_i(\pm\lambda) = \rho_i^{(0,0)} \pm \lambda\rho_i^{(1,0)}$, the exchange–correlation kernel is obtained by numerical symmetric differentiation.
- (67) Vosko, S. H.; Wilk, L.; Nusair, M. Accurate Spin-Dependent Electron Liquid Correlation Energies for Local Spin-Density Calculations: A Critical Analysis. *Can. J. Phys.* **1980**, *58*, 1200–1211.
- (68) Cohen, R. E.; Cvitas, T.; Frey, J. G.; Holmström, B.; Kuchitsu, K.; Marquardt, R.; Mills, I.; Pavese, F.; Quack, M.; Stohner, J.; et al. *Quantities, Units and Symbols in Physical Chemistry: IUPAC Green Book*, 3rd ed.; IUPAC & RSC Publishing: Cambridge, U.K., 2008.
- (69) Strictly speaking, the nonrelativistic g-tensor shift (in the absence of SO effects) is 0. However, we will keep this notation in order to stay consistent with the work of Rastrelli and Bagno,³² from which the data were taken. The NR results in Table 4 thus refer to methods in which SO effects are taken into account perturbationally.